

CONF-880110--25

Los Alamos National Laboratory is operated by the University of California for the United States Department of Energy under contract W-7405-ENG 36

TITLE APPLICATION OF PULSE COMPRESSION AND SHAPING TO THE FEL PHOTOELECTRIC INJECTOR

AUTHOR(S) Dinh C. Nguyen, CLS-6
David E. Watkins, CLS-6
Michael E. Weber, CLS-6

SUBMITTED TO SPIE, for Proceedings of the meeting held in Los Angeles, CA on January 11-16, 1988

DISCLAIMER

This report was prepared as an account of work sponsored by an agency of the United States Government. Neither the United States Government nor any agency thereof, nor any of their employees, makes any warranty, express or implied, or assumes any legal liability or responsibility for the accuracy, completeness, or usefulness of any information, apparatus, product, or process disclosed, or represents that its use would not infringe privately owned rights. Reference herein to any specific commercial product, process, or service by trade name, trademark, name, or otherwise does not necessarily constitute an endorsement, recommendation, or favoring by the United States Government. The views and opinions of authors expressed herein do not necessarily state or reflect those of the United States Government or any agency thereof.

By acceptance of this article the publisher recognizes that the U.S. Government retains a nonexclusive, royalty-free license to publish or reproduce the published form of this contribution or to allow others to do so for U.S. Government purposes.

The Los Alamos National Laboratory requests that the publisher identify this article as work performed under the auspices of the U.S. Department of Energy.

Los Alamos Los Alamos National Laboratory
Los Alamos, New Mexico 87545

Application of Pulse Compression and Shaping to the FEL Photoelectric Injector

**Dinh C. Nguyen, David E. Watkins and Michael E. Weber
Los Alamos National Laboratory, Los Alamos, NM 87545**

ABSTRACT

We discuss the application of self-phase modulation and grating pulse compression to the generation of temporally trapezoidal optical pulses for controlling the electron beam emittance and energy spread in an FEL photoelectric injector. Pulse compression in a single-stage pulse compressor, with background reduction based on the nonlinear birefringence of the optical fiber, yields 3-ps, compressed pulses without background pedestals or sidelopes. Trapezoidal, flat-topped pulses with 20-ps FWHM and 4-ps risetime have been obtained through self-phase modulation and group-velocity dispersion of the 3-ps pulses in a second fiber. Pulse shaping through Fourier transform amplitude and phase masking in the frequency domain and the amplification of the trapezoidal pulses are also discussed.

1. INTRODUCTION

The recent advent of the photoelectric injector - an electron injector design based on laser photocathode emitters - has generated a considerable amount of interest because of the high electron beam brightness achievable from this injector.¹⁻⁵ High current density, low beam emittance and small energy spread have recently been demonstrated for the photoelectric injector incorporating a Cs₃Sb photoemitter in an RF cavity, as illustrated in Fig. 1.³⁻⁵ This design also lends itself to control of the electron beam emittance and energy spread by programming the temporal and spatial formats of the photocathode illumination by the modelocked laser pulses. Theoretical simulations⁶ predict that for a space-charge dominated electron beam, minimum beam emittance and energy spread are obtained if the electron bunch has uniform current density, both radially and axially. Thus, the ideal illumination temporal and spatial pulse format is a flat top with steep edges. In this paper, we describe a method to generate short, 20-ps optical pulses with a trapezoidal, flat-topped pulse shape from a Nd:YAG modelocked laser.

2. PULSE COMPRESSION WITH BACKGROUND REDUCTION

Using the fiber-grating pulse compression technique,^{7, 8} we compressed the output of a cw modelocked Nd:YAG laser operating at 100 MHz repetition

rate from 100 ps to 3 ps. The experimental setup for pulse compression is shown in Fig. 2. In order to assure stable and reproducible pulse compression, a permanent magnet Faraday rotator was inserted between the laser and the pulse compressor to isolate the reflection off the front surface of the fiber or any stimulated backward Rayleigh scattering from interfering with the laser modelocking operation. A half-wave plate/polarizer combination served as a variable attenuator to allow continuous adjustment of laser power into the fiber. The role of the second half-wave plate and subsequent retarders are described later.

Through self-phase modulation (SPM) in the 25-m non-polarization preserving fiber (NRC F-SV with a 5 μ core diameter), the 100-ps optical pulses developed a frequency spread of ~ 10 cm^{-1} . With this fiber length, the positive group velocity dispersion (GVD) of the fiber did not change the pulse width appreciably. The average laser power incident on the fiber was approximately 5 W but only 60% of that exited the fiber, presumably due to coupling loss at the input of the fiber. The chirped pulses were compressed to 3-ps FWHM in a double-pass grating arrangement with a 1700 grooves/mm diffraction grating. The compressed pulse width was measured with a non-collinear, background-free SHG autocorrelator.

For a gaussian pulse shape, the theoretical compressed pulsewidth is given by

$$t_{\text{FWHM}} = \frac{3.77}{\Delta\omega} \quad (1)$$

where $\Delta\omega$ is the frequency spread produced by SPM in the fiber. In the absence of positive GVD, $\Delta\omega$ can be approximated by

$$\Delta\omega = \frac{K L n_2 \omega P}{c A_{\text{eff}} t_{\text{FWHM}}} \quad (2)$$

where $K = 2(2\ln 2)^{1/2} e^{-1/2} \sim 1.428$ for gaussian pulses

$$n_2 = 6.2 \times 10^{-20} \text{ m}^2/\text{W} \quad (1.1 \times 10^{-13} \text{ esu})$$

$$P = P_{\text{av}} / (1.12 f_r t_{\text{FWHM}})$$

and $A_{\text{eff}} = 1.26 \pi D^2/4$; D and L are the fiber core diameter and length, respectively. Taking 3 W as an estimate of the laser power inside the fiber, we calculate a frequency chirp of ~ 7.5 cm^{-1} and a compressed pulse width of 2.8 ps, in good agreement with the observed width.

For efficient and stable pulse compression, the laser peak power must be below the critical power of stimulated Raman scattering, P_C .

$$P_C \sim \frac{k A_{\text{eff}}}{G L_i} \quad (3)$$

where $k = 32$ for non-polarization preserving fiber⁹

$G =$ the peak Raman gain (9.2×10^{-14} m/W)

and $L_i =$ the effective interaction length

The calculated P_C for a 25-m non-polarization preserving fiber is 344 W, or an average power of 3.9 W, putting us well below threshold.

The use of short fibers allows generation of compressed pulses with appreciable output power without the complication of stimulated Raman scattering. However, in the absence of positive GVD, the chirps produced in short fibers are nonlinear, resulting in pedestals and sidelopes in the background of the compressed pulses (Fig. 3a). These unwanted features can be reduced by a spectral windowing method which removes the offending frequencies which are at the extremes of the frequency distribution and occur in time at the leading and trailing edges of the pulses.¹⁰ Alternatively, the nonlinear birefringence of the fibers can be used to enhance the contrast ratio of the central part of the pulse with respect to the background.¹¹ We will show that by using the fiber nonlinear birefringence to perform spectral windowing, the background can be reduced without introducing the sidelopes that result from the sharp edges of the spectral windows.

As shown in Fig. 2, our implementation of the nonlinear background reduction method is simpler than that described in Ref. [11]. The half-wave plate immediately in front of the fiber allows rotation of the plane polarized laser light to maximize the nonlinear birefringence in the optical fiber, giving maximum intensity-dependent rotation. At the exit of the fiber, the input plane polarized light is elliptically polarized due to the fiber linear birefringence. The nonlinear birefringence rotates the major axes of the ellipses through an angle dependent upon the light intensity, and hence time-dependent. A quarter-wave plate at the output end converts these elliptically polarized light at the peak intensity back to plane polarized light. A second half-wave plate is used to rotate the polarization to the p-polarization of the diffraction grating. The diffraction grating has a contrast ratio of better than 2 between the p- and s- polarizations and 4

diffraction passes increase the contrast ratio to 16. With a proper orientation of the entrance and exit half-wave plates, the low-intensity background of the chirped pulses is substantially reduced, and hence the unwanted frequency components are suppressed. The resulting compressed pulses are void of the pedestal or sidelopes, as shown in Fig. 3b.

The chirps produced in the absence of GVD are linear in the middle of the optical pulses.⁷ The low-intensity background of the chirped pulses contains extraneous frequencies which cannot be recompressed by the grating pair. By removing the low-intensity background, we have also rejected these extraneous frequency components. This analysis is supported by the two spectra of the compressed pulses with and without background reduction shown in Fig. 4. The compressed pulses without background reduction have a familiar spectral distribution of $\sim 10 \text{ cm}^{-1}$, with two "horns" at the edges of the distribution, whereas the pulses with background reduction have a somewhat narrower (FWHM = 8 cm^{-1}) and smoother spectral distribution. This method of spectral windowing does not introduce sharp edges which can cause sidelopes.

3. GENERATION OF TRAPEZOIDAL PULSES

The background-free 3-ps pulses were used to generate trapezoidal pulses by propagation in a second, 55-m fiber where additional SPM increased the bandwidth of the pulses to $\sim 50 \text{ cm}^{-1}$. With this combination of fiber length and bandwidth, GVD becomes significant, and the pulses stretch into a trapezoidal shape, as previously reported by Nakatsuka *et al.*¹² The amount of pulse stretching can be estimated by

$$\Delta t = \frac{L \Delta \nu D(\lambda)}{c \nu} \quad (4)$$

where $D(\lambda) = 0.011$ at 1.064μ . For $\Delta \nu = 50 \text{ cm}^{-1}$ and $L = 55 \text{ m}$, we obtained a flat-topped region of about 10 ps in width, or 13 ps FWHM of the trapezoidal pulses, slightly less than the observed pulsewidth.

Figure 5a illustrates a background-free SHG cross-correlation trace of the trapezoidal pulse with the 3-ps pulse. The cross-correlated pulse shape exhibits no background and a very good stability. The leading and trailing edges are rounded off by the 3-ps pulsewidth of the probe pulse. Further

compression of the trapezoidal pulses in a second grating pair yielded 500-fs pulses but with substantial background. The cross-correlation trace of the trapezoidal pulses probed with the 500 fs pulses is shown in Fig. 5b. The background in this cross-correlation trace is higher due to a non-zero background in the probe pulses and the large ratio between the widths of the trapezoidal and the probe pulses. As measured in this cross-correlation trace, the trapezoidal pulses have a 4-ps risetime (10%-90%) and a 15-ps flat-topped region, in reasonable agreement with prediction given the inaccuracy in determining the peak power and effective core area. As previously observed in Ref. [12], the autocorrelation of the trapezoidal pulses (Fig. 5c) is a triangular waveform whose base width is twice the trapezoidal pulse basewidth.

Another method for generating the square pulses is Fourier transform phase and amplitude masking in the frequency domain.^{13, 14} This technique offers the advantages of requiring a smaller frequency spread and having the flexibility of programming the pulse shape. The drawback of this method is that it necessitates fabrication of complex amplitude and phase masks that cannot be easily modified. One possibility is to replace the lithographically generated amplitude masks with the limited bandwidth of an amplifier gain medium used to amplify the pulses after compression and pulse shape synthesis.

The amplification of the generated trapezoidal pulses requires large bandwidth gain media such as Nd:YLF or Nd:glass. Gain narrowing of the bandwidth at high amplification distorts the pulse shape. In the case of Nd:YAG, silicate glass amplifiers are better matched to the 1.064 μ central wavelength. Preliminary calculations show that negligible distortion in the pulse shape will be introduced if phosphate glass is used as the amplifier medium for Nd:YLF and silicate glass for Nd:YAG.

3. CONCLUSION

A temporally trapezoidal pulse shape with ~20 ps FWHM has been obtained via self-phase modulation and positive group velocity dispersion in a two-stage fiber-grating pulse compression and shaping technique. The average power of trapezoidal pulses is about 0.2 W, yielding a peak power is of about 100 W. The double-stage arrangement yields the desired pulse shape without significant stimulated Raman scattering in the fiber and with relatively low loss of optical power. Amplification of these trapezoidal

pulses may require the use of large bandwidth gain media such as phosphate and silicate glasses. The new temporal pulse format applied to the photocathode could produce electron bunches which are better synchronized with the accelerating RF field and exhibit a more uniform space charge. We thus expect to significantly improve the beam emittance and energy spread of the electron beams generated in a photoelectric injector.

4. ACKNOWLEDGEMENTS

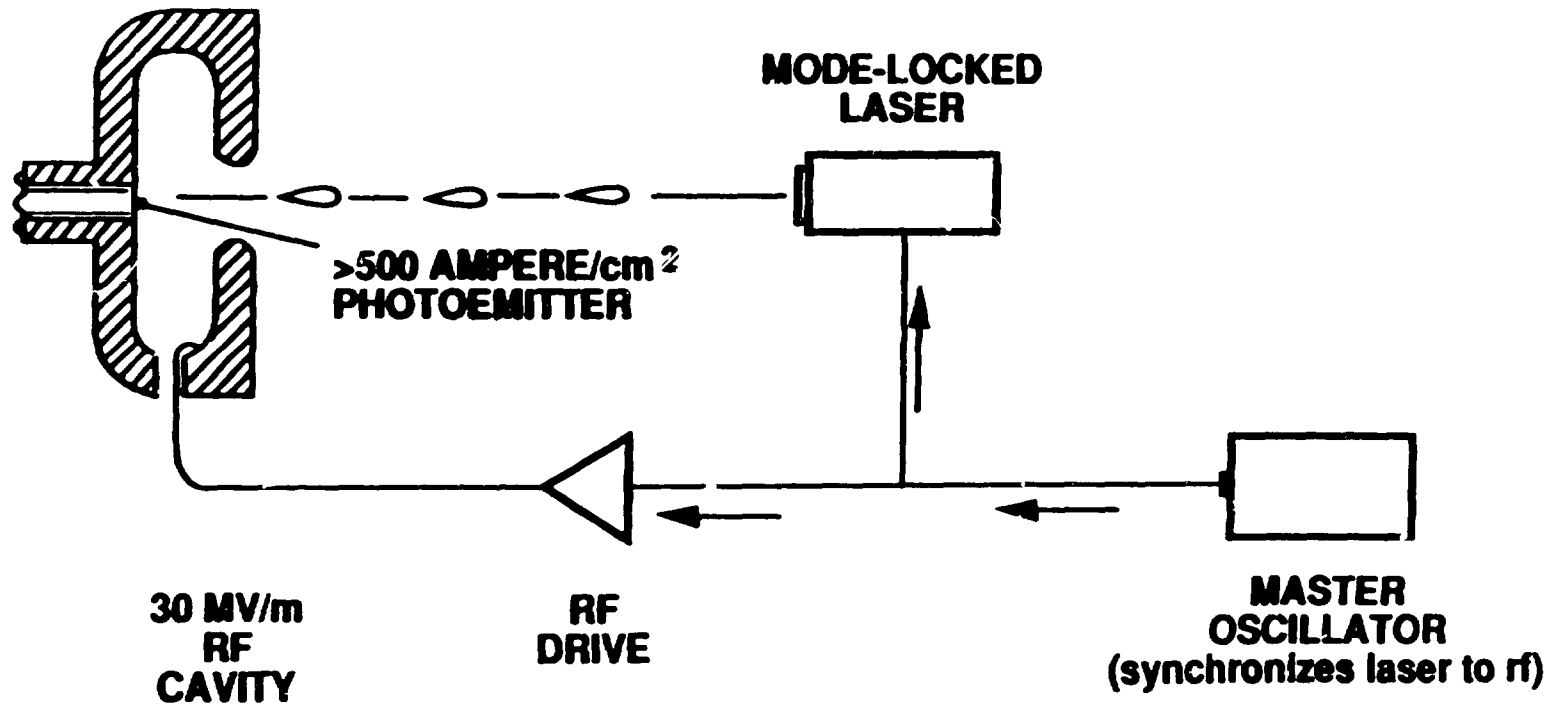
The authors thank Norman Kurnit and David Moore for helpful discussions and suggestions. This work was performed under the auspices of the US Department of Energy and supported by the US Army Strategic Defense Command.

5. REFERENCES

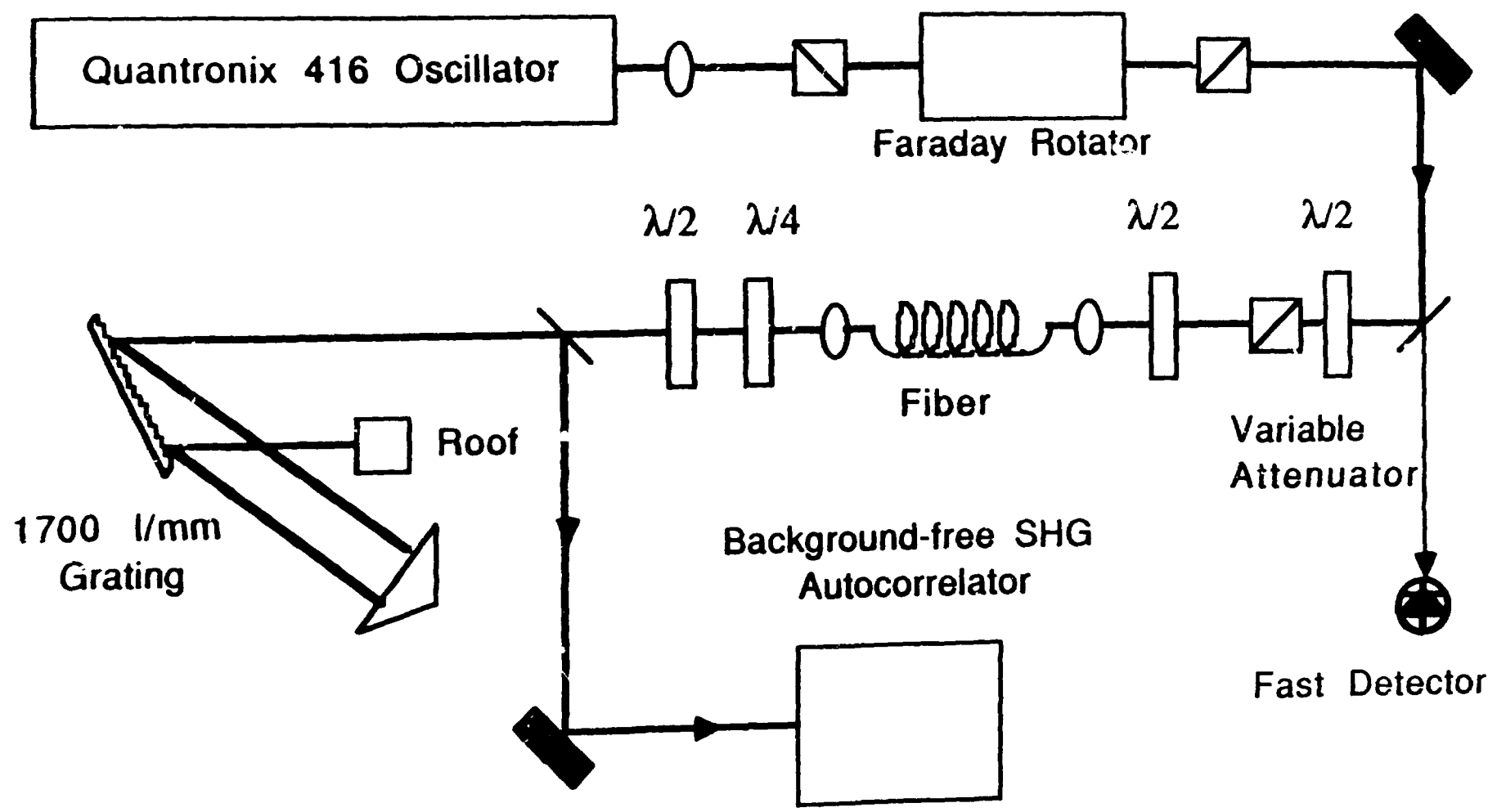
1. C. H. Lee "High current density photoemissive electron source," Appl. Phys. Lett. **44**, 565 (1984)
2. C. H. Lee, P. E. Oettinger, E. Purg, R. Linostein, J. Jacob, J. S. Fraser, and R. L. Sheffield, "Electron emission of over 200 A/cm² from a pulsed-laser irradiated photocathode," IEEE Trans. Nucl. Sci., **32** (5), 3045 (1985)
3. J. S. Fraser, R. L. Sheffield, E. R. Gray, and G. W. Rodenz, "High-brightness photoemitter injector for electron accelerator," Proc. 1985 Particle Accelerator Conference, LA-UR 85-1603.
4. J. S. Fraser, R. L. Sheffield, and E. R. Gray, "A new high-brightness electron injector for Free-Electron Laser driven by RF linacs," Proc. 7th Int. Free Electron Laser Conf.
5. J. S. Fraser, R. L. Sheffield, E. R. Gray, P. M. Giles, R. W. Springer, and V. A. Loeb, "Photocathodes in accelerator applications," 1987 Particle Accelerator Conference, LA-UR 87-863, to be published.
6. M. E. Jones and W. Peter "Theory and simulation of high-brightness electron beam production from laser-irradiated photocathodes in the presence of DC and RF electric fields," Proc. 6th Int. Conf. on High-Power Particle Beams, Kobe, Japan, June 1986, LA-UR 86-1941.

7. W. J. Tomlinson, R. H. Stolen, and C. V. Shank "Compression of optical pulses chirped by self-phase modulation in fibers," J. Opt. Soc. Am. B1 (2), 139 (1984).
8. C. V. Shank, R. L. Fork, R. Yen, R. H. Stolen, and W. J. Stolen "Compression of femtosecond optical pulses," Appl. Phys. Lett. 40, 761 (1982).
- 9.
10. J. P. Heritage, R. N. Thurnston, W. J. Tomlinson, A. M. Weiner, and R. H. Stolen "Spectral windowing of frequency-modulated optical pulses in a grating compressor," Appl. Phys. Lett. 47(2), 87 (1985).
11. N. J. Halas, and D. Grischkowsky "Simultaneous optical pulse compression and wing reduction," Appl. Phys. Lett. 48(13), 823 (1986)
12. H. Nakatsuka, D. Grischkowsky, and A. C. Balant "Nonlinear picosecond-pulse propagation through optical fibers with positive group-velocity dispersion," Phys. Rev. Lett. 47(13), 910 (1981).
13. J. P. Heritage, A. M. Weiner, and R. N. Thurnston "Picosecond pulse shaping by spectral phase and amplitude manipulation," Opt. Lett. 10(12), 609 (1985).
14. A. M. Weiner, J. P. Heritage, and R. N. Thurnston "Synthesis of phase-coherent, picosecond optical square pulses," Opt. Lett. 11(3), 153 (1986).

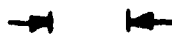
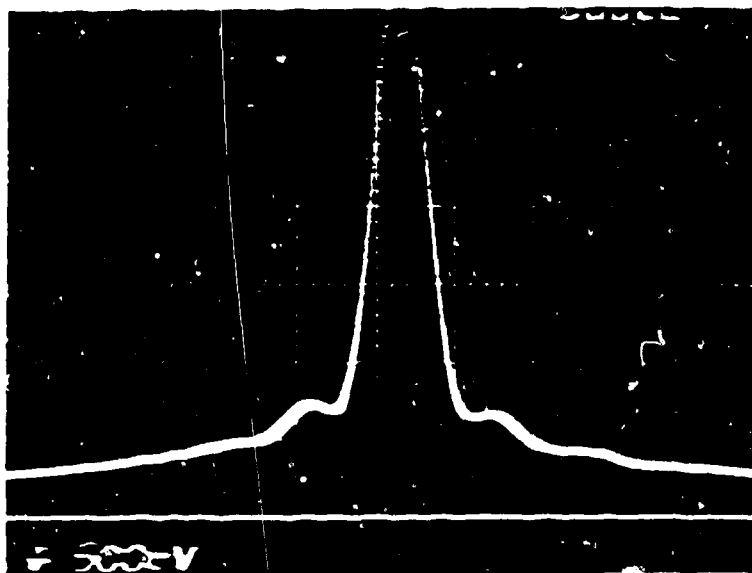
**NEW DESIGN APPROACH MINIMIZES EMITTANCE
GROWTH BY ELIMINATING BUNCHERS
AND ACCELERATING RAPIDLY**



BLOCK DIAGRAM OF FIBER-GRATING PULSE COMPRESSION WITH NONLINEAR BIREFRINGENCE BACKGROUND REDUCTION



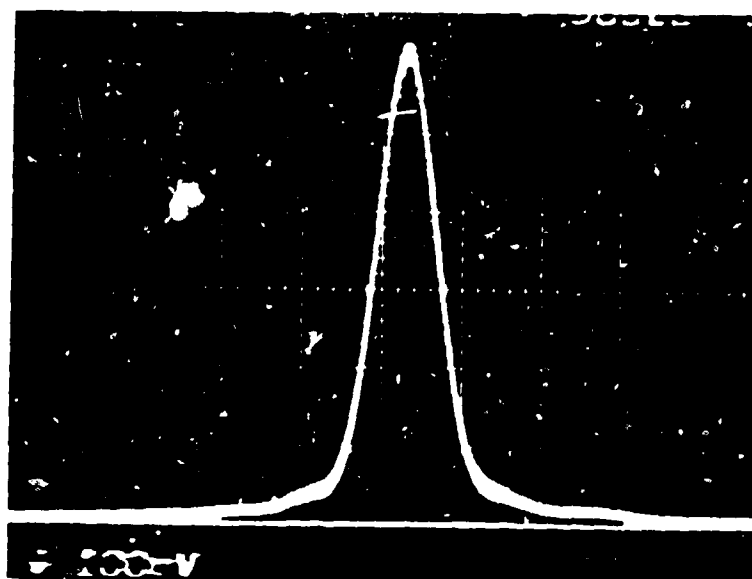
**AUTOCORRELATION TRACE OF THE 3-ps, COMPRESSED PULSE
WITHOUT BACKGROUND REDUCTION**



3.5 ps

Fig 3a

**AUTOCORRELATION TRACE OF THE 3-ps, COMPRESSED PULSE
WITH BACKGROUND REDUCTION**



→ ←

3.5 ps

Fig. 3b

Plot of WIRESPEC.inten vs WIRESPEC.cn

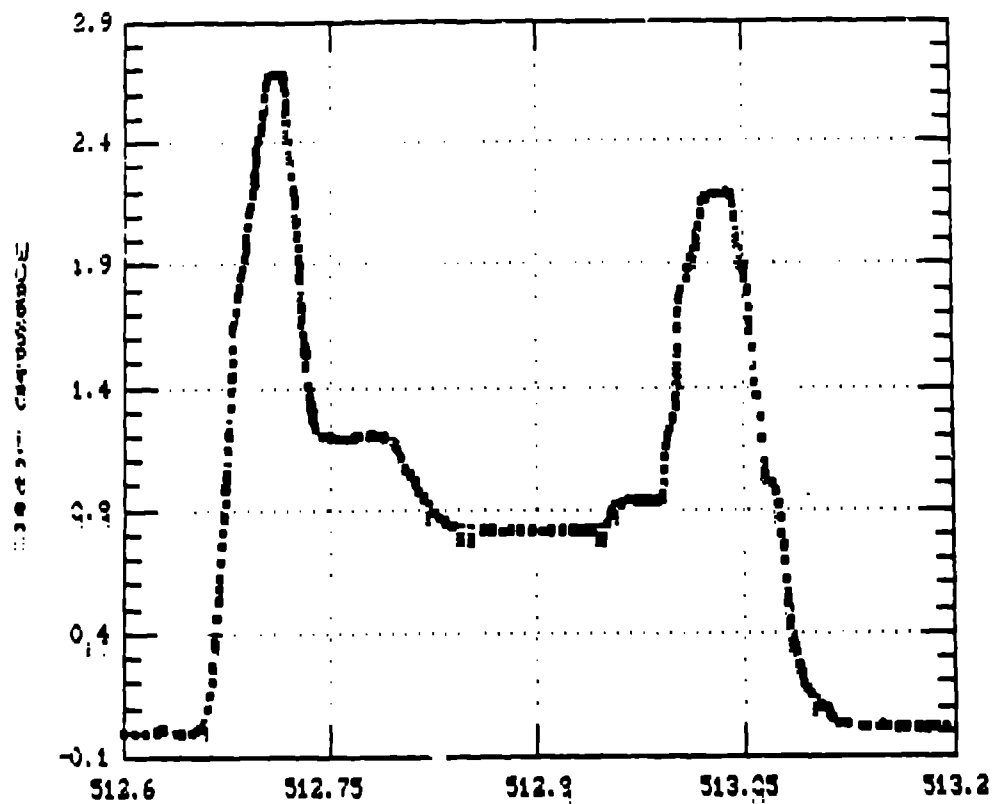


Fig 4a

Plot of WIRESPEC.inten vs WIRESPEC.cn

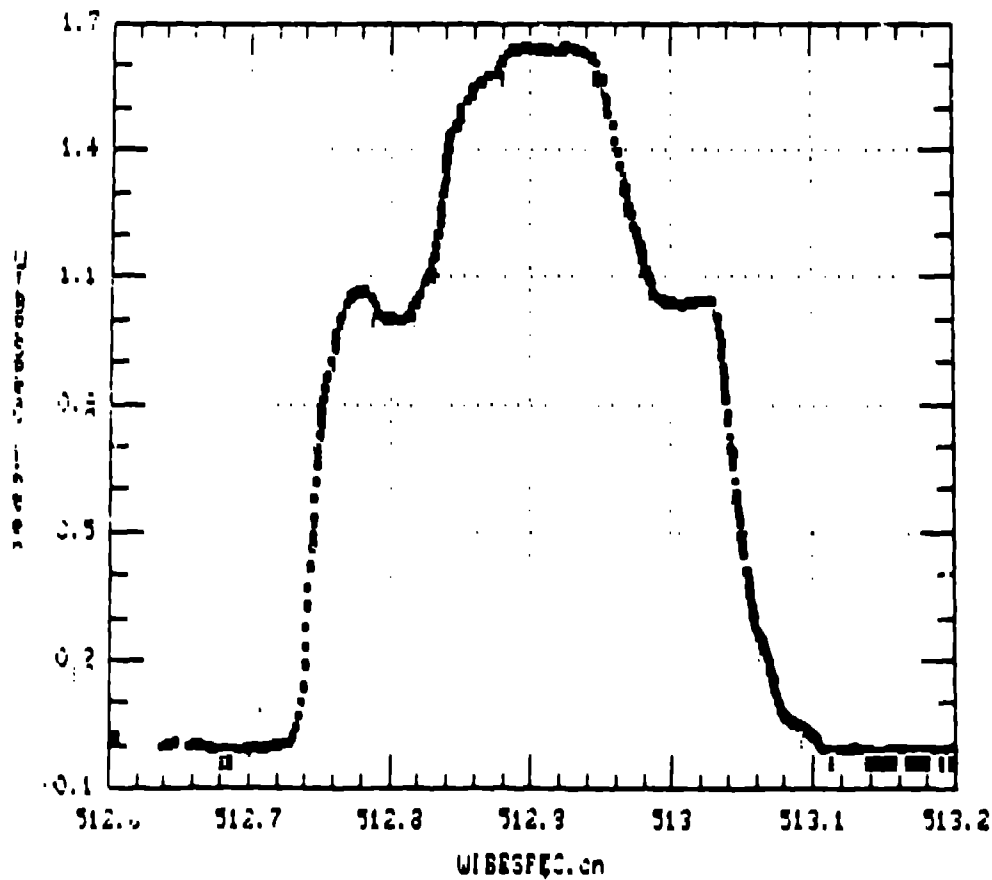


Fig 4b

**CROSS-CORRELATION TRACE OF THE 15-ps, TRAPEZOIDAL PULSE
WITH THE 3-ps PROBE PULSE**

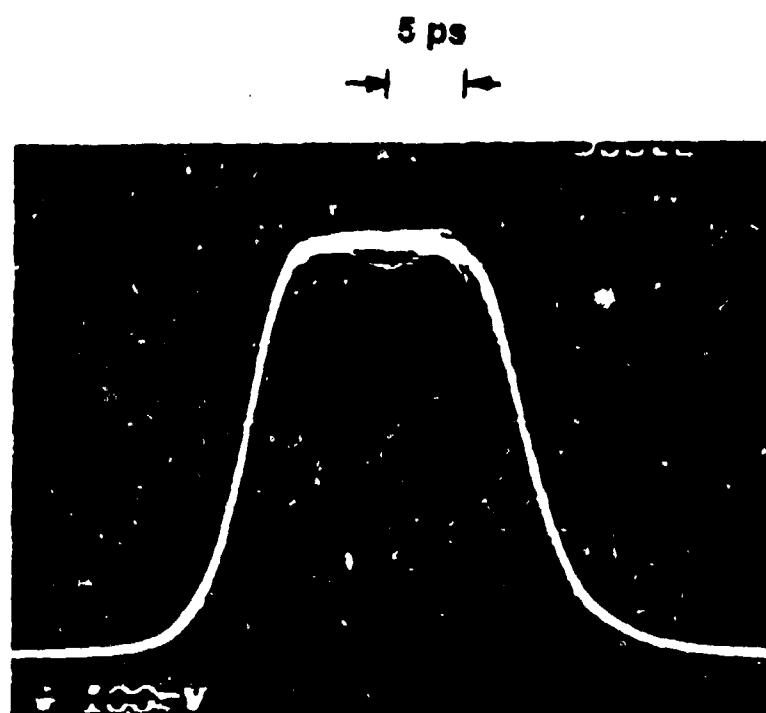
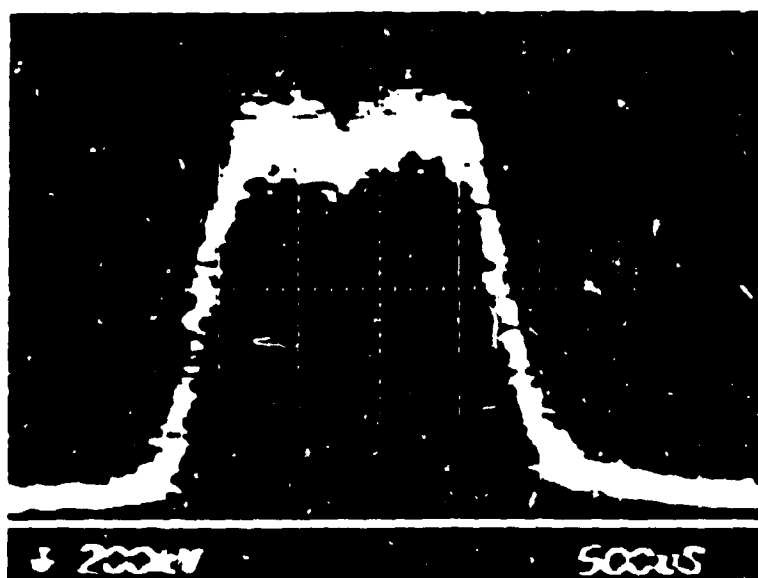


Fig 5a

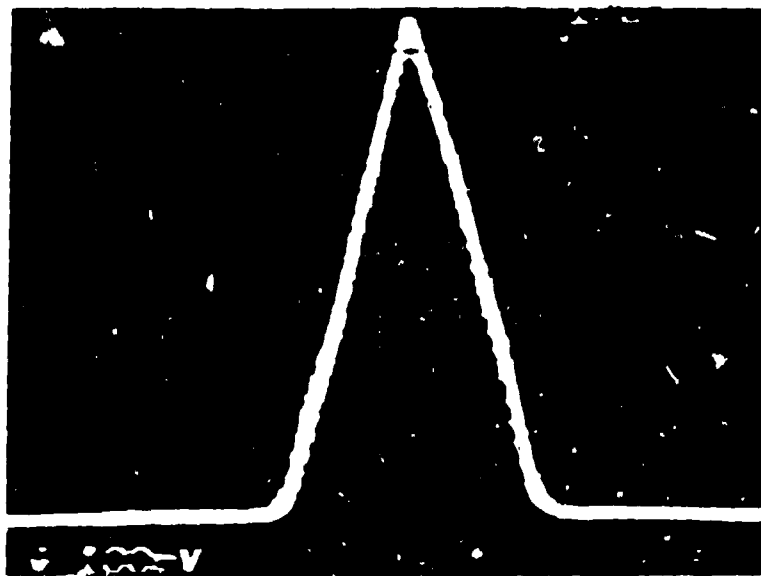
**CROSS-CORRELATION TRACE OF THE 15-ps, TRAPEZOIDAL PULSE
WITH THE 600-fs PROBE PULSE**



—| |—
5 ps

F. y 5 b

AUTOCORRELATION TRACE OF THE 15-ps, TRAPEZOIDAL PULSE



← →
10 ps

Fig 5c